3

Rotor Design for High-Speed Flywheel Energy Storage Systems

Malte Krack[1], Marc Secanell[2] and Pierre Mertiny[2]
[1]*Institute of Dynamics and Vibration Research, Gottfried Wilhelm Leibniz Universität Hannover*
[2]*Department of Mechanical Engineering, University of Alberta*
[1]*Germany*
[2]*Canada*

1. Introduction

1.1 Kinetic energy storage using flywheels

Devices employing the concept of kinetic energy storage date back to ancient times. Pottery wheels and spinning wheels are early examples of systems employing kinetic energy storage in a rotating mass. With the advent of modern machinery, flywheels became commonplace as steam engines and internal combustion engines require smoothing of the fluctuating torque that is produced by the reciprocating motion of the pistons of such machines.

More recently, flywheel systems were developed as true energy storage devices, which are also known as mechanical or electromechanical batteries. A remarkable example of such a system was the sole power source of the 'Gyrobus' - a city bus that was developed by the Maschinenfabrik Oerlikon in Switzerland in the 1930's, see Motor Trend (1952). This vehicle contained a rotating flywheel that was connected to an electrical machine. At regular bus stops, power from electrified charging stations was used to accelerate the flywheel, thus converting electrical energy to mechanical energy stored in the flywheel. When traveling between bus stops, the electrical machine gradually decelerated the flywheel and thus converted mechanical energy back to electricity, which was used to power the electrical motor driving the bus. The disk-shaped flywheel rotor was made of steel, had a mass of about 1.5 metric tons and reached a maximum angular velocity of 314 rad/s or 3000 rounds per minute (rpm). In regular operation, deceleration of the flywheel was limited to about half of the maximum disk speed. The amount of energy thus made available allowed the Girobus to travel for a distance of up to 6 km in regular traffic.

Contemporary flywheel energy storage systems, or FES systems, are frequently found in high-technology applications. Such systems rely on advanced high-strength materials as flywheels usually operate at speeds exceeding 10,000 rpm. Vacuum enclosures and magnetic bearing systems are frequently employed to minimize energy losses due to friction. Only through the use of advanced technology have FES systems become commercially viable for a range of applications, causing FES research and development to be an active and rapidly evolving field.

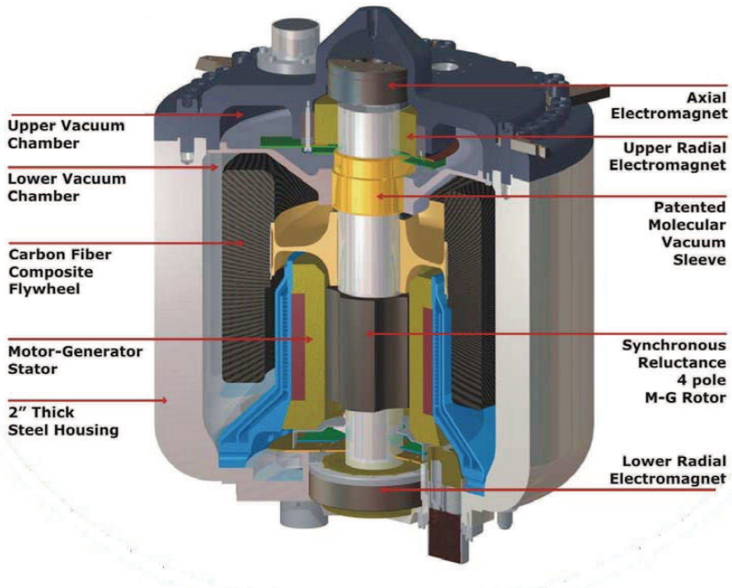

Fig. 1. Example of a commercial flywheel energy storage system (courtesy of POWERTHRU, Livonia, MI, USA - www.power-thru.com)

1.2 FES applications and industrial significance

FES systems and electrochemical batteries can be designed to have comparable energy storage capacities. But, FES systems offer superior energy discharge rates which are considerably higher than in comparable electrochemical battery systems. This characteristic makes FES systems attractive for certain applications. FES systems may provide a cost-effective means in cases where stand-by and rapidly engaging power supply is required. For example, FES units can be used as an uninterruptable power supply (UPS) to protect data centers from grid power failures, cf. Brown & Chvala (2005). For the same reasons FES technology is becoming increasingly popular as a means of ensuring reliable electricity supply to consumers (Bornemann & Sander (1997); Tarrant (1999)). An example of a commercial flywheel energy storage system is shown in **Figure 1**. The installation of clusters of FES units provides for power capacity in the megawatt-level, which enables electrical utilities to perform fast-response regulation of the grid frequency. FES technology lends itself to a range of similar applications, such as peak power support in off-grid industrial systems and energy supply management infrastructure involving renewable energy sources (wind and solar power).

Examples of FES systems given in the preceding section can be categorized as stationary applications. Interest in such systems is presently considerable, yet even greater attention has been given to the development mobile FES systems over the last decades. Even more so than rapid energy charge and discharge capabilities, the comparatively high specific power, i.e. power per unit mass makes FES systems highly attractive for applications in which the mass of the energy storage unit is of substantial importance. Space applications have traditionally been at the forefront of research and development activities in this context, see e. g. Christopher & Donet (1998). More recently, emerging segments in the automotive field, such as highly energy efficient and hybrid vehicles have become another area of applications. So-called kinetic energy recovery systems (KERS) are currently under development for use primarily in motorsports. A cutaway model of a KERS unit is shown in **Figure 2**, which reveals the flywheel rotor. In conjunction with an advanced mechanical transmission this

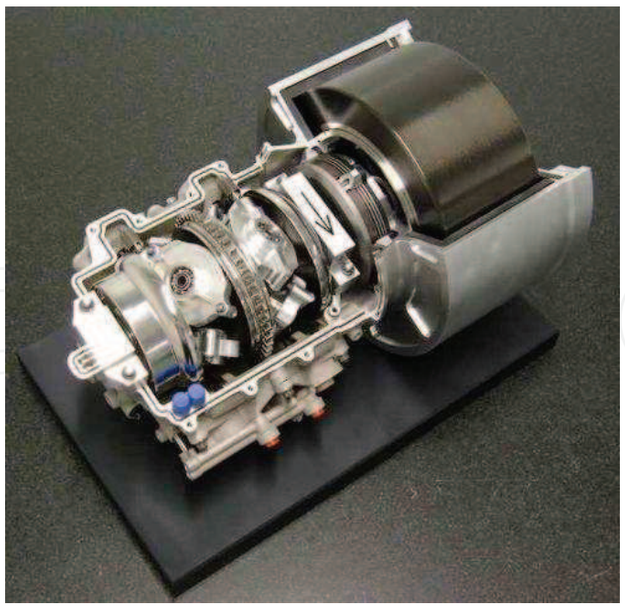

Fig. 2. Flywheel in a Kinetic Energy Recovery System (KERS) (courtesy of Flybrid Systems LLP, Silverstone, Northamptonshire, England

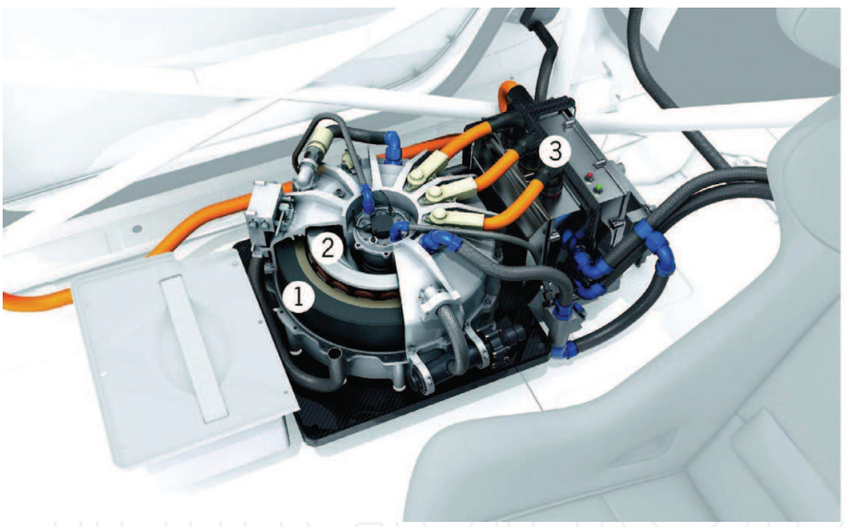

Fig. 3. FES system in a high-performance hybrid automobile (courtesy of Dr. Ing. h.c. F. Porsche AG, Stuttgart, Germany)

flywheel rotor is able to reach top speeds around 60,000 rpm. The energy storage and power capacity of the shown unit with mass of 25 kg is 400 kJ and 60 kW respectively. It is important to note that this and other KERS devices do not necessarily involve energy conversion from electrical to mechanical, and vice versa; instead, mechanical energy is transferred directly to the flywheel rotor using advanced transmission systems. Conversely, electrical-mechanical energy conversion is often required for hybrid vehicles. Shown in **Figure 3** is the electromechanical battery unit for a high-performance hybrid automobile.

1.3 Advantages and disadvantages of FES systems

Several advantages are associated with the use of FES systems compared to electrochemical batteries. Most commonly cited are the superior power and excellent energy capacity per system mass of FES units. The specific power of many FES systems ranges between 5 and 10 kW/kg whereas values for electrochemical batteries are typically smaller by one order of magnitude. The specific energy of advanced FES systems may exceed 200 Wh/kg (Arnold et al. (2002)), and values of 100 Wh/kg are commonly achieved. Specific energies of electrochemical systems are usually around 30 Wh/kg for lead-acid batteries and in excess of 100 Wh/kg for lithium-ion batteries. The situation is different when comparing FES technology to electrochemical batteries on a cost basis. Compared to lead-acid battery systems, an up to eight times higher purchase cost per amount of energy stored can be expected for FES systems (Hebner et al. (2002)). However, the considerably higher price of FES systems is offset by their significant longer life, which may exceed that of electrochemical batteries by the same factor. In this context it is often emphasized that FES units can sustain a practically unlimited number of charge/discharge cycles without reductions in energy storage capacity, whereas for electrochemical batteries the number of charge/discharge cycles is limited due to decreasing battery performance. Cost consideration also must include the storage system's energy recovery efficiency. Modern FES units are 90 to 95% efficient whereas corresponding values for electrochemical batteries are typically much lower, i.e. 60 to 70% for lead-acid batteries. Other advantages of FES technology are a lesser environmental impact due to the absence of harmful chemicals that are usually part of electrochemical batteries, and the ability of FES units to operate effectively over a wide temperature range; electrochemical batteries perform effectively only within a relatively narrow temperature band.

1.4 Basic working principle

The central part of every FES unit is the flywheel rotor. When set in rotation the rotor acquires angular momentum and stores mechanical energy. The rotor is accelerated or decelerated by an electrical machine, usually a combined motor/generator unit. Note that also mechanical systems are used for this purpose in some applications (e.g. the aforementioned KERS). As mentioned above, flywheel rotors usually rotate at high angular velocities. Magnetic bearings and vacuum enclosures are therefore often used to minimize frictional losses that occur in the bearings and with the air surrounding rotating components, respectively. The typical components of advanced FES cells are shown in **Figure 1**. The energy stored in the rotor is increased by accelerating the rotor to higher speeds, i.e. the FES is being charged. In electromechanical systems, the rotor is accelerated by the electrical machine operating in motor mode. When required the energy stored in the rotor can be released by operating the electrical machine in generator mode producing electricity. Conditioning of the electrical power to or from the motor/generator unit is achieved by power electronic systems. **Figure 4** illustrates the power flow affecting flywheel rotor rotation for the charge and discharge cycle.

1.4.1 Kinetic energy

The kinetic energy stored in a flywheel rotating with an angular velocity ω is given by the following equation:

$$E_{\text{kin}} = \frac{1}{2} I \omega^2 , \tag{1}$$

where I is the mass moment of inertia of the rotating components. Assuming a cylindrical rotor made from a single material with density ϱ, and having an inside and outside radius of

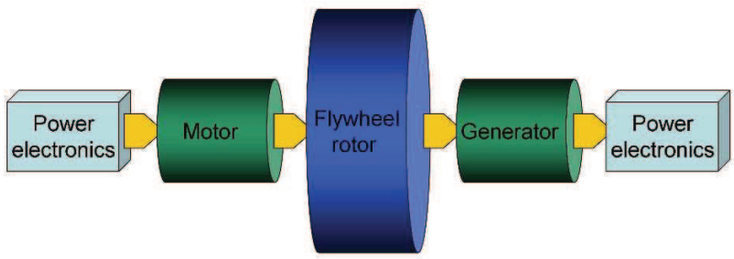

Fig. 4. Schematic showing power flow in FES system

r_i and r_o and a height of h, a further expression for the kinetic energy stored in the rotor can be determined as

$$E_\mathrm{kin} = \frac{1}{4}\varrho\pi h(r_\mathrm{o}^4 - r_\mathrm{i}^4)\omega^2\,. \tag{2}$$

From the above equation it can be deduced that the kinetic energy of the rotor increases quadratically with angular velocity, and hence high rotational speeds are desirable. The equation also shows that the rotor diameter has an even greater influence on kinetic energy. One must however consider the constraint that mechanical strength of the rotor material imposes on the rotor diameter and angular velocity. Considering a thin rim rotor as an approximation, it can be shown that the product of maximum rotor radius and angular velocity is dependent on the square root of the specific strength of the rotor material, i.e.,

$$r_\mathrm{o,max}\omega = \sqrt{\frac{S_{\Theta\Theta}}{\varrho}}\,, \tag{3}$$

where $S_{\Theta\Theta}$ is the strength of the material in circumferential or hoop direction. Hence, rotors are preferably made from low density, high strength fiber-reinforced polymer composite (FRPC) materials that are filament-wound in circumferential direction.

1.4.2 Flywheel configurations

An important aspect of flywheel design, in addition to rotor material selection and dimensioning, is the structure connecting the rotor to the electrical machine. Such a structure also needs to support the rotor within the housing of the FES unit. It is common to connect the rotor via a hub to a rotating shaft that is supported by bearings. In these cases the electrical machine is either directly connected to the hub, or it drives the rotor using the common shaft. In other designs the electrical machine is integrated into the rotor hub structure.

During rotor rotation, centrifugal forces generate stresses in the circumferential as well as in the radial direction. As hoop tensile stresses are dominant, high material strength is required for this direction. In composite flywheel rotors this is accomplished by circumferentially aligning the fiber reinforcement phase. Hoop stresses are not uniform along the rotor radius. For rotors made from a single material the maximum tensile hoop stress is to be expected on the inside of the rotor, see e. g. Krack et al. (2010c). The rotation induced loading thus causes a mismatch in rotor growth creating tensile stresses in the radial direction. Since fiber composite rotors generally lack reinforcement in the radial direction, causing low strength transverse to the fiber direction, rotors are more likely to fail due to cracking of the polymer phase (delamination) rather than fiber breakage (Tzeng et al. (2005)). A central part of

rotor design is therefore the reduction of radial tensile stresses. Researchers have proposed and implemented several solutions to this design problem based on material selection and manufacturing considerations, which will be discussed in subsequent sections.
An appropriately designed hub structure may also reduce radial stresses in flywheel rotors. This is accomplished by providing a compliant hub structure that due to the action of centrifugal forces superimposes compressive loading in the radial direction. Ha et al. (2006) proposed a hub structure that is split at multiple locations along its length. Hub segments are therefore able to impose the desired radial compressive load on the inside of the rotor.

1.5 Objectives in flywheel design

The design of FES units usually follows two different yet related objectives. For applications in which the FES unit is part of a mobile system, e.g. automobile or spacecraft, designers strive to maximize specific kinetic energy of the flywheel for given constraints and requirements. Such an approach implies incorporating rotor materials with maximum specific strength, which is usually associated with high cost. For stationary FES systems in e.g. UPS and utility applications, the energy storage capacity and not the mass of the flywheel are typically an important design factor. Such systems are usually of considerable size, requiring large volumes of material, and material cost is therefore an additional key design consideration. Flywheel design based on cost considerations is a rather new approach, which will be described further in subsequent parts of this article.

2. Flywheel rotor manufacturing

2.1 Filament winding

Filament winding is the most common manufacturing technique for flywheel rotors. In this method filamentous reinforcement is wrapped circumferentially onto suitable mandrels creating a rotor rim with high hoop strength. The reinforcement phase is embedded in a polymer matrix, which is applied along with the fibers either as a liquid phase (wet winding), semisolid or solid phase (i.e. winding of towpreg or prepreg material). In the latter cases the polymer phase must usually be liquefied upon deposition by heating to enable fiber consolidation. Thermoset polymer matrices such as epoxies are common for these processes, but alternative polymers such as elastomers have also been employed successfully (Gabrys & Bakis (1997)). Thermoset polymer phases further require curing, typically at elevated temperatures, which may occur after or even during the winding process. Elevated temperature curing may induce residual thermal stresses, which can affect the radial tensile strength of a composite rotor. Hence, thermal effects need to be considered during rotor design. Following the filament winding process the rotor rim may require removal of the winding mandrel and machining to specific tolerances.

2.2 Rotor composition and assembly

Flywheel rotors can be filament-wound as a single material, single rim rotor. Rotor and hub may be assembled by interference fit to mitigate aforementioned radial tensile stresses during flywheel operation. An interference fit is frequently produced by appropriately heating and cooling the rotor and hub to exploit thermal expansion effects for the assembly. By varying fiber tensioning during filament winding some additional compressive radial pre-stressing of the rotor may be achieved.
Although the manufacture of thick single rim rotors is feasible, such designs generally result in suboptimal energy storage capacity. Rotors with a large ratio of outside to inside

radius were found to provide only limited radial tensile strength (Arvin & Bakis (2006)). Better performance can be achieved by assembling a rotor from several individual rims of the same material by mechanical press-fit, thermal shrink-fit and pressurized adhesion (Ratner et al. (2003)). In this manner a compressive radial pre-stressing of the rotor can be tailored that enables the flywheel to operate at higher rotational speeds without failure; greater energy storage capacity is thus achieved.

A hybrid rotor structure consisting of multiple rings made from different fiber and/or resin materials may further reduce radial tensile stresses, see Genta (1985); Portnov (1989). Rotor performance was shown to improve by placing rims with higher material density and/or lower YOUNG modulus on the inside radius of the rotor (promoting increased expansion of these rims in radial direction during flywheel rotation). Conversely, rims with progressively lower density and higher modulus should be located toward the outside of the rotor (constraining radial displacement) (Ha, Kim & Choi (1999)). Similarly, a tailoring method called 'ballasting' was proposed for reducing radial tensile stresses and attaining a more uniform stress field in the rotor. In this method, the ratio of hoop YOUNG modulus to mass density, $\frac{E_{\Theta\Theta}}{\varrho}$, is increased along the outward radial direction of the flywheel rotor by tailoring fiber winding angles and/or the type of fiber material with respect to the radial position. 'Ballasting' may even include low modulus regions that contain resin with little or no reinforcement. To further mitigate the risk of failure, a polymer phase with high strain to failure and reduced YOUNG modulus may be considered. However, highly radial compliant rotors may become susceptible to adverse dynamic behavior. Incorporating compliant elastic or elastomeric interlayers between rims was also shown to improve rotor performance. This approach aims at inhibiting the transmission of radial stress between rims, thus relieving radial stresses.

To overcome the problem of circumferential crack propagation in filament-wound flywheel rotors, Gowayed et al. (2002) discussed flywheel configurations containing reinforcement fibers in the circumferential as well as the radial direction. In the same manner, rims may be made of so-called polar woven composites (Huang (1999)). In this approach, rims are composed of a circular or spiral weave incorporating fibers in the radial and circumferential directions to achieve a balance between radial and hoop strength. Limitations for this type of rotor were found to arise from failures in resin-rich zones and matrix cracking induced by fiber kinking and ensuing high local stresses.

3. Modeling

During service, the flywheel rotor undergoes large rotational speeds, typically in the range of $10,000$ to $100,000$ rmp. Moreover, the rotor is subjected to fast charge and discharge operations. Thus, the load spectrum of a flywheel rotor is characterized by large static centrifugal loading as well as transient accelerating/braking load. In order to perform an accurate stress analysis, the interaction with the surrounding components, in particular the flywheel hub, is also of importance.

The stress distribution has a significant impact on the failure criteria that represent nonlinear constraints of the design optimization problem formulated in Section 4. Simplified analytical and finite element (FE) approaches exist in order to calculate the stress distribution within the rotor and they are presented in Subsections 3.1 and 3.2, respectively. Remarks concerning the benefits of either approach are given in Subsection 3.3. Since multi-rim rotors of different fiber reinforced polymer composites are state-of-the-art technology, this chapter focuses on this type of rotor design.

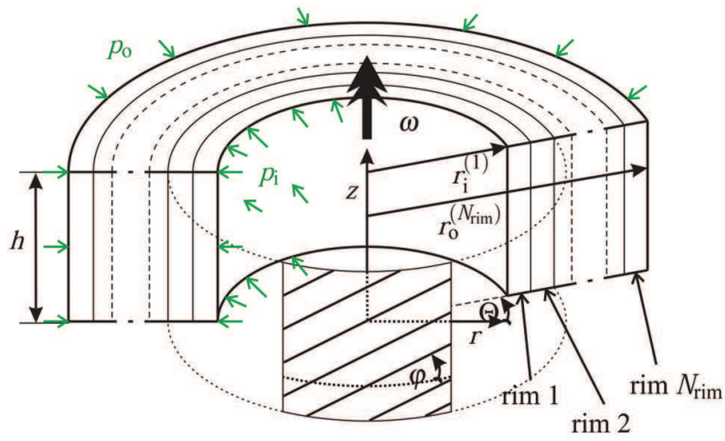

Fig. 5. Multi-rim setup of the flywheel rotor

3.1 Analytical approaches

In **Figure 5**, a multi-rim flywheel rotor is illustrated. Its geometry is typically modeled as axially symmetric. This assumption appears sound since the balancing in terms of achieving axisymmetry is an important objective in the manufacturing of a flywheel rotor. Danfelt et al. (1977) was one of the first to publish an analytical method of analysis for a hybrid composite multi-rim flywheel rotor with rim-by-rim variation of transversely isotropic material properties. The method presented in this subsection generalizes DANFELT's approach in terms of its various extensions. Thorough validation of the method by means of FE analysis and experiments is given in references Ha et al. (2003); Ha & Jeong (2005); Ha et al. (2006).

To the authors' knowledge all publications regarding analytical solutions to the described problem assume a constant rotational velocity. Hence, the transient behavior of charging and discharging operations which might indirectly limit the allowable maximum rotational speed, cannot be accounted for. The local equation of equilibrium in the radial direction of the cylindrical coordinate system for purely centrifugal loading due to the rotational velocity ω reads as

$$\frac{\partial \sigma_{rr}}{\partial r} + \frac{1}{r}\left(\sigma_{rr} - \sigma_{\Theta\Theta}\right) + \varrho\omega^2 r = 0\,. \tag{4}$$

For typical strains in flywheel applications, the nonlinearity of the FRPC material behavior can be neglected. Thus, a linear relationship between stress $\boldsymbol{\sigma}$, strain $\boldsymbol{\varepsilon}$ and temperature ΔT can be stated,

$$\boldsymbol{\sigma} = \boldsymbol{Q}\left(\boldsymbol{\varepsilon} - \boldsymbol{\alpha}\Delta T\right)\,. \tag{5}$$

Herein, $\boldsymbol{\alpha}$ is the vector of thermal expansion coefficients and $\boldsymbol{Q}$ is the global stiffness matrix. The stresses and strains are written as vectors of generally six elements of the symmetric stress tensor in cylindrical coordinates. The stress vector therefore comprises the three normal stresses $\sigma_{rr}, \sigma_{\Theta\Theta}, \sigma_{zz}$ and the the shear stresses $\sigma_{\Theta z}, \sigma_{zr}, \sigma_{r\Theta}$. Using the temperature difference ΔT, the effect of residual stresses from the curing process can be studied, see Ha et al. (2001).

Viscoelasticity can also be considered by means of the analytical modeling. This effect may have a significant influence on the long-term stress state within the flywheel rotor. Tzeng et al. (2005); Tzeng (2003) investigated this effect by transforming the thermoviscoelastic problem into its corresponding thermoelastic problem in the LAPLACE space. The resulting thermoelastic relationship is similar to Eq. (5) and can thus be solved in an analog manner, cf. reference Tzeng (2003) for details. It was shown, however, by Tzeng et al. (2005)

that stress relaxation occurs when time progresses. Thus, the constraining state which has to be considered in the optimization procedure is the initial state so that effects of thermoviscoelasticity are not considered in the following.
Only unidirectional laminates shall be studied. Thus, transversely isotropic material behavior is assumed. Ha et al. (1998) were one of the first authors to investigate effects of varying fiber orientation angles on optimum rotor design. For this type of lay-up, the fiber direction does not coincide with the circumferential direction so that the local and the global coordinate systems are not identical. The global stiffness matrix $\boldsymbol{Q}$ then has to be computed from the local stiffness matrix $\bar{\boldsymbol{Q}}$ by means of a coordinate transformation,

$$\boldsymbol{Q} = \boldsymbol{T}^{\mathrm{T}}(\psi)\bar{\boldsymbol{Q}}\boldsymbol{T}(\psi)\,. \tag{6}$$

The local stiffness matrix $\bar{\boldsymbol{Q}}$ only depends on the material properties and can be assembled e. g. using the well-known five engineering constants for unidirectional laminates (Tsai (1988)),

$$\bar{\boldsymbol{Q}} = \bar{\boldsymbol{Q}}(E_1, E_2, G_{12}, \nu_{12}, \nu_{23})\,. \tag{7}$$

Typically, the rotor geometry qualifies for a reduction of the independent unknowns in terms of a plain stress or a plain strain assumption. It is thus possible to obtain a closed-form solution of the structural problem (Ha et al. (1998); Krack et al. (2010c); Fabien (2007)). The assumption of plain stress is valid only for thin rotors ($h \ll r_\mathrm{i}$), whereas thick rotors ($h \gg r_\mathrm{i}$) can be treated with a plain strain analysis.
Assuming small deformations, the quadratic terms of the deformation measures can be neglected, resulting in a linear kinematic. The relationship between the radial displacement distribution u_r and the circumferential and radial strains holds,

$$\varepsilon_{\Theta\Theta} = \frac{u_r}{r}\,, \quad \varepsilon_{rr} = \frac{\partial u_r}{\partial r}\,. \tag{8}$$

Substitution of Eqs. (5)-(8) into Eq. (4) yields the governing equation for u_r, which represents a second-order linear inhomogeneous ordinary differential equation with non-constant coefficients. A closed-form solution is derived in detail in reference Ha et al. (2001). Since the governing equation depends on the material properties, the solution is only valid for a specific rim.
The unknown constants of the homogeneous part of the solution for each rim are determined by the boundary and compatibility conditions, i. e. the stress and the displacement state at the inner and outer radii of each rim j, ${r_\mathrm{i}}^{(j)}$ and ${r_\mathrm{o}}^{(j)}$ respectively. Regarding compatibility, it has to be ensured that the radial stresses are continuous along the rim interfaces of the N_rim rims, whereas the radial displacement may deviate by an optional interference $\delta^{(j)}$,

$$\sigma_{r_\mathrm{i}}^{(j+1)} = \sigma_{r_\mathrm{o}}^{(j)}\,, \qquad \text{for } j = 1(1)N_\mathrm{rim} - 1 \quad \text{and} \tag{9}$$

$$u_{r_\mathrm{i}}^{(j+1)} = u_{r_\mathrm{o}}^{(j)} + \delta^{(j)}\,, \quad \text{for } j = 1(1)N_\mathrm{rim} - 1\,. \tag{10}$$

The effect of interference fits $\delta^{(j)}$ was studied in reference Ha et al. (1998).
It has to be noted that the continuity of radial stresses implies that the rims are bonded to each other. This is generally not the case for an interference fit since mating rims are usually fabricated and cured individually. Hence, no tensile radial stresses can be transferred at the

interface. A computed positive radial stress would mean detachment failure in this case. Therefore, the general analytical model does not take care of implausible results so that the results have always to be regarded carefully.
The required last two equations are obtained from the radial stress boundary conditions at the innermost and outermost radius of the rotor

$$\sigma_{r_\mathrm{i}}^{(1)} = p_\mathrm{in}\,, \quad \sigma_{r_\mathrm{o}}^{(N_\mathrm{rim})} = -p_\mathrm{out}\,. \tag{11}$$

The pressure at the outermost rim p_out is typically set to zero, the inner pressure p_in can be used to consider the interaction with the flywheel hub. The conventional ring-type hub can simply be accounted for as an additional inner rim. It should be noted that the typically isotropic material behavior of a metallic hub can easily be modeled as a special case of transversal isotropy. A split-type hub was studied in reference Ha et al. (2006). Therefore, the inner pressure was specified as the normal radial pressure caused by free expansion of the hub,

$$p_\mathrm{in} = \omega^2 \varrho_\mathrm{hub} \frac{\left(r_\mathrm{i}^{(1)}\right)^3 - \left(r_\mathrm{i}^{(\mathrm{hub})}\right)^3}{3\left(r_\mathrm{i}^{(1)}\right)}\,. \tag{12}$$

In the generalized modified plain strain assumption used in reference Ha et al. (2001), a linear ansatz for the axial strain was chosen. Thus, two additional constraints were introduced: The resulting force and moment caused by the axial stress for the entire rotor was set to zero. According to Ha et al. (2001), the linear ansatz for the axial strain yielded better results than its plain stress or plain strain counterparts in comparison to the FE analysis results.
In conjunction with the solution, the compatibility and boundary conditions can be compiled into a real linear system of equations for the $N_\mathrm{rim} + 1$ unknown constants of the solution. It can be shown that the system matrix is symmetric for a suitable preconditioning described in reference Ha et al. (1998). Once solved, the displacement and stress distribution can be evaluated at any point within the rotor.

3.2 Numerical approaches

In comparison to the analytical approaches, finite element (FE) approaches offer several benefits in terms of modeling accuracy. For a general three dimensional or two dimensional axisymmetric FE analysis, a plain stress or strain assumption is not necessary. Furthermore nonlinearities can be accounted for, including the contacting interaction of rotor and hub, the nonlinear material behavior and the nonlinear kinetmatics in case of large deflections. Also, more complicated composite lay-ups other than the unidirectional laminate could be modeled. Another advantage is the capability of examining the effect of transient accelerating or braking operations on the load configuration of the rotor.
In order to provide insight into the higher accuracy of the numerical model, the radial and circumferential stresses for a two-rim rotor similar to the one presented by Krack et al. (2010b) is illustrated in **Figures 6(a)-6(b)**. The rotor consists of an inner glass/epoxy and an outer carbon/epoxy rim and is subjected to a split-type hub (not shown in the figure).
It should be noted that apart from the non-axisymmetric character of the stress distributions, the stress minima and maxima are no longer located at the same height. This indicates that optimization results that are only based on plain stress or strain assumptions and axial symmetry should at least be validated numerically. It has to be remarked that the normal stress in the axial direction and the shear stresses, which are not depicted, are generally

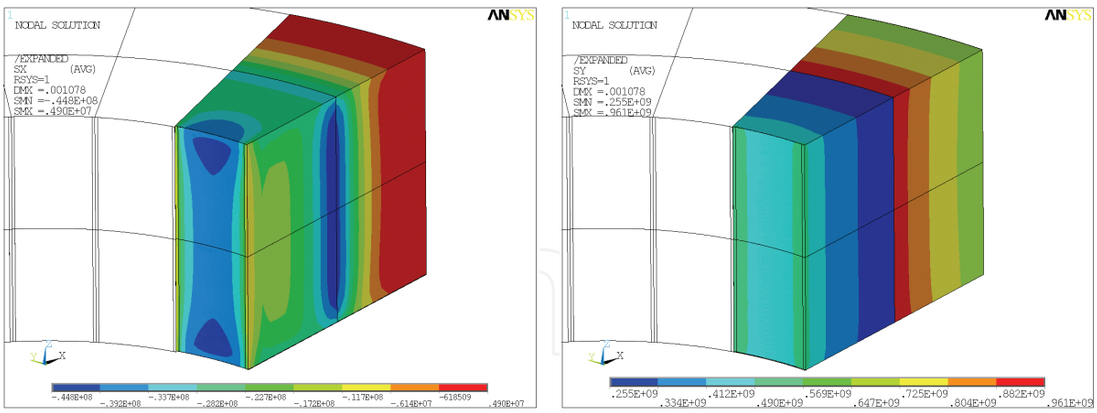

(a) Radial stress σ_{rr} in $\mathrm{N/m^2}$ (b) Circumferential stress $\sigma_{\Theta\Theta}$ in $\mathrm{N/m^2}$

Fig. 6. Stress distributions in the finite element sector model for a rotational speed of $n = 30000\ \mathrm{min}^{-1}$

non-zero which cannot be accurately predicted by the analytical model.
Despite the higher accuracy of the numerical model, comparatively few publications can be found in the literature concerning the design of hybrid composite flywheels using numerical simulations. Ha, Kim & Choi (1999) developed an axisymmetric finite element and employed it to find the optimum design of a flywheel rotor with a permanent magnet rotor. Takahashi et al. (2002) examined the influence of a press-fit between a composite rim and a metallic hub employing a contact simulation technique in an FE code. Gowayed et al. (2002) studied composite flywheel rotor design with multi-direction laminates using FE analysis. In Krack et al. (2010b), both an analytical and an FE model were employed in order to predict the stress distribution within a hybrid composite flywheel rotor with a nonlinear contact interaction to a split-type hub.

3.3 Remarks on the choice of the modeling approach

The main benefit of the analytical model is that it is much less computationally expensive. Since there are typically several orders of magnitude between the computational times of analytical and numerical approaches, this advantage becomes a significant aspect for the optimization procedure (Krack et al. (2010b)). Some optimization strategies, in particular global algorithms require many function evaluations and would lead to an enormous computational effort in case of using an FE model. The choice of the model thus not only affects the optimum design but also facilitates optimization. On the other hand, the FE approach facilitates a greater modeling depth and flexibility, since there is no need for the simplifying assumptions that are necessary to obtain a closed-form solution in the analytical model.
Owing to the capability of greater modeling depth, numerical methods gain importance for the design optimization of flywheel rotors. If effects such as geometric, material and contact nonlinearity or complex three-dimensional loading need to be accounted for in order to achieve a sufficient accuracy of the model, the FE analysis approach renders indispensable. Furthermore, increasing computer performance diminishes the significant disadvantage of more computational costs in comparison to analytical methods. Methods that combine the benefits of both approaches are discussed in Subsection 4.4.

4. Optimization

Various formulations for the design optimization problem of the flywheel rotor have been published. A generalized formulation reads as

$$\begin{aligned} &\text{Maximize} && f(\boldsymbol{x}) = f\left(E_{\text{kin}}(\boldsymbol{x}), M(\boldsymbol{x}), D(\boldsymbol{x}), \cdots\right) \\ &\text{with respect to} && \boldsymbol{x} = \{\text{set of geometric variables, rotational speed, material properties}\} \\ &\text{subject to} && \text{structural constraints} \quad \text{and} \\ & && \boldsymbol{x}_{\min} \leq \boldsymbol{x} \leq \boldsymbol{x}_{\max} \end{aligned} \quad . \tag{13}$$

Thus, the objective of the design problem is to maximize a function generally depending on the kinetic energy stored E_{kin}, the mass M and the cost D. The design variables can be any subset of all geometric variables, rotational speed and material properties. The optimum design is always constrained by the strength of the structure. In addition, bounds for the design variables might have to be imposed. The concrete formulation of the design problem strongly depends on the application, manufacturing opportunities and other design restrictions. Different suitable objective function(s) are discussed in Subsection 4.1, common design variables are addressed in Subsection 4.2 and constraints are the topic of Subsection 4.3. Depending on the actual formulation of the design problem, an appropriate optimization strategy has to be employed, see Subsection 4.4.

4.1 Objectives

Regardless of the application, all objectives for FES rotors are energy-related. The total kinetic energy stored in the rotor can be expressed as

$$E_{\text{kin}} = \frac{1}{2} I_{zz} \omega^2 \,, \tag{14}$$

where I_{zz} is the rotational mass moment of inertia. It was assumed that the rotation of the flywheel is purely about the z-axis with a rotational velocity ω.
For small deflections, I_{zz} can approximately be calculated considering the undeformed structure only,

$$I_{zz} = \frac{1}{2} \sum_{j=1}^{N_{\text{rim}}} m_j \left[\left(r_{\text{o}}^{(j)}\right)^2 + \left(r_{\text{i}}^{(j)}\right)^2 \right] = \frac{\pi}{2} h \sum_{j=1}^{N_{\text{rim}}} \varrho_j \left[\left(r_{\text{o}}^{(j)}\right)^4 - \left(r_{\text{i}}^{(j)}\right)^4 \right] , \tag{15}$$

with the masses m_j, the rotor height h and the constant density ϱ_j of each rim. It becomes evident from Eq. (14) that the kinetic energy increases quadratically with the rotational speed ω and only linearly with the inertia I_{zz}. The inertia of the outer rims has more influence on the kinetic energy than the one in the inner rims. It should be noted that in typical FES applications the total energy is not the most relevant parameter, instead the difference between the maximum energy stored and the minimum energy stored, i. e. the energy that can be obtained by discharging the FES cell from its bound rotational velocities $\omega_{\max}$ and $\omega_{\min}$ is relevant.
Another important aspect is the minimization of the rotor weight. This is particularly significant for mobile applications. The total mass M of the rotor reads as

$$M = \sum_{j=1}^{N_{\text{rim}}} m_j = \pi h \sum_{j=1}^{N_{\text{rim}}} \varrho_j \left[\left(r_{\text{o}}^{(j)}\right)^2 - \left(r_{\text{i}}^{(j)}\right)^2 \right] . \tag{16}$$

In case of stationary applications, it might be even more critical to minimize the rotor cost. Therefore, the total cost D (Dollar) has to be calculated,

$$D = \pi h \sum_{j=1}^{N_{\text{rim}}} d_j \varrho_j \left[\left(r_{\text{o}}^{(j)} \right)^2 - \left(r_{\text{i}}^{(j)} \right)^2 \right] . \tag{17}$$

Herein, the weighting factors d_j are the price per mass values of each material. Thus, it is assumed that the total cost can be split up into partitions that can directly be associated with the mass of each material. It should be noted that these prices are often hardly available in practice and are subject to various influences such as the manufacturing expenditure and the required quantities. The former aspect is usually strongly influenced by the complexity of the rim setup, i. e. the number of rims and optional features such as interference fits. Conclusions directly drawn from an optimization for an arbitrarily chosen set of prices should therefore be regarded as questionable. In Krack et al. (2010c) and Krack et al. (2010a), the optimization is therefore performed with the price as a varying parameter.

Naturally, trade-offs between the main objectives have to be made. A large absolute energy value can only be achieved by a heavy and expensive rotor. Minimizing the cost or the weight for a given geometry would result in selecting the cheapest or lightest material only. However, the benefits of hybrid composite rotors, i. e. rim setups using different materials in each rim have been widely reported.

In order to obtain a design that exhibits both requirements, i. e. a large storable energy and a low mass or cost, it is intuitive to formulate the optimization problem as a dual-objective problem with the objectives energy and mass or energy and cost. As an alternative, the ratio between both objectives can be optimized in order to achieve the largest energy for the smallest mass/cost, resulting in a single-objective problem. The ratio between energy and mass is also known as the specific energy density SED,

$$SED = \frac{E_{\text{kin}}}{M} . \tag{18}$$

The energy-per-cost ratio reads as follows:

$$ECR = \frac{E_{\text{kin}}}{D} . \tag{19}$$

The following discussion regarding single- and multi-objective design problem formulations addresses the trade-off between storable energy and cost. However, the statements generally also hold for the goal of minimizing the mass instead of the cost.

Solving optimization problems with multiple objectives is common practice for various applications with conflicting objectives, (e. g. Secanell et al. (2008)). The solution of a multi-objective problem is typically not a single design but an assembly of so called PARETO-optimal designs. In brief, PARETO-optimality is defined by their attribute that it is not possible to increase one objective without decreasing another objective. The dual-objective approach thus covers a whole range of energy and cost values associated to the optimal designs. This is the main benefit compared to a single-objective optimization with the energy-per-cost ratio as the only objective, which only has a single optimal design. It is generally conceivable that this design with the largest possible energy-per-cost value might exceed the maximum cost, or its associated kinetic energy could be too low for a practical application.

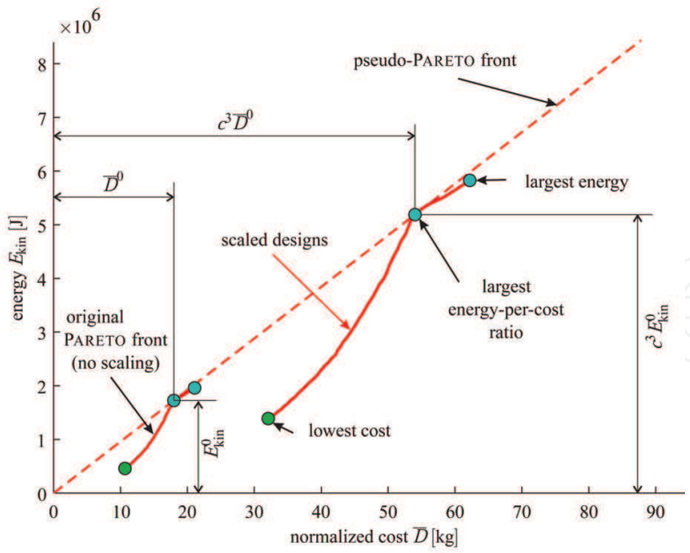

Fig. 7. Reduction of the multi-objective to a single-objective design problem using the scaling technique

For the particular mechanical problem of a rotor with a purely centrifugal loading and linear materials, however, Ha et al. (2008) showed that any flywheel design can be linearly scaled in order to achieve a specified energy or cost/mass value. Due to the linearity of Eqs. (4)-(8), the stress distribution remains the same if all geometric variables are scaled proportionally and the rotational velocity inversely proportional to an arbitrary factor c. After scaling, the energy, ${E_{\text{kin}}}^0$, and cost, D^0, of the original optimal design would increase by the factor c^3 so that the energy-per-cost value ${E_{\text{kin}}}^0/D^0 = c^3{E_{\text{kin}}}^0/(c^3D^0)$ is also constant. This design scaling is illustrated in **Figure 7**. If scaling is possible, i. e., the total radius of the rotor is not constrained, then, scaling can be used in order to achieve a rotor that always has the maximum energy-per-cost ratio. Therefore, if scaling is possible, all other points in the PARETO fronts in **Figure 7** would be suboptimal compared to scaling the design in order to achieve the maximum energy-per-cost ratio. A new PARETO front for the dual-objective design problem in conjunction with the scaling technique would therefore be a line through the origin with the optimal energy-per-cost value as the slope. This pseudo-PARETO front is also depicted in **Figure 7** (dashed line). If size is constrained, other points in the PARETO set will have to be considered for the given geometry. It should be noted that it is assumed that scaling opportunity still holds approximately also for nonlinear materials and large deformations within practical limits. It is also important to remark that there are more established and computationally efficient numerical methods for the solution of single-objective design problems than for multi-objective problems. Therefore, the single-objective problem formulation should be preferred if the mechanical problem and the constraints of the problem Eq. (13) allow this. In the following, it shall be assumed that this requirement holds. Hence, the specific energy density or the energy-per-cost ratio can be applied in a single-objective design problem formulation. For problems where mass and cost are of inferior significance, it is also common to optimize the total energy stored as the only objective, $\boldsymbol{f} = E_{\text{kin}}$.

It should be noted that there is generally no set of design variables that maximizes all of the objectives but there are different solutions for each purpose (Danfelt et al. (1977)). The

total energy stored was considered as objective in Ha, Yang & Kim (1999); Ha, Kim & Choi (1999); Ha et al. (2001); Gowayed et al. (2002). The trade-off between energy and mass, i. e. maximization of the specific energy density SED was addressed in the following publications: Ha et al. (1998); Arvin & Bakis (2006); Fabien (2007); Ha et al. (2008). Particularly for stationary energy storage applications, the aspect of cost-effectiveness might be more relevant. Krack et al. (2010c); Krack et al. (2010b); Krack et al. (2010a) addressed this economical aspect by maximizing the energy-per-cost ratio ECR.

4.2 Design variables

Various design variables have been investigated for the optimization of the composite rotor and hub design for FES. A list of the most relevant design variables is given below:

- Rotational speed
- Material properties (E_{ij}, ν_{ij}, ϱ)
- Interferences
- Fiber direction angle
- Rim thicknesses
- Rotor height
- Hub design

Many design variables directly influence the rim setup. It was shown in Ha, Yang & Kim (1999) that a lay-up with radially increasing hoop stiffness to density ratio $\frac{E_{\Theta\Theta}}{\varrho}$ is most beneficial in terms of energy capacity. An increasing value $\frac{E_{\Theta\Theta}}{\varrho}$ ensures that the outer part of the rotor prevents the inner part from expanding. Thus, the radial stresses tend to be compressive during operation, and the more critical tensile stresses across the fiber are reduced.

Apparently this type of rim setup can be achieved by designing the material properties in a suitable manner. Discrete combinations of rims with piecewise constant material properties, i. e. hybrid composite rotors are state-of-the art. By using different materials in the same rotor, the hoop stiffness as well as the density can be varied. A continuously varying fiber volume fraction is also conceivable but more complex in terms of design and manufacturing. Due to anisotropy, the hoop stiffness can also be decreased by winding the fibers not circumferentially but with a non-zero fiber angle (fiber angle variation).

The overall radial stress level can also be decreased by introducing interferences between adjacent rims. It should be noted that interferences are also necessary in order to accomplish compressive interface stresses for the torque transmission within the rotor. By adapting the hub design, e. g. by employing a split-type hub, the strength of the rotor can also be increased, as it will be shown later in this subsection.

Naturally the rotational speed is also a common variable that influences not only the kinetic energy stored but also increases the centrifugal loading. Thus, there exists a critical rotational speed for any type of rotor. However, the rotational speed is different from the design variables discussed above in that it varies with service conditions. Consequently, the rotational speed can be treated as a design variable or a constant parameter that determines the size of the flywheel design in terms of the scaling technique as in Ha et al. (2008), see Subsection 4.1. In fact, for the case of a single-material rotor with constant inner and outer radii, the rotational speed could also be treated as an objective in order to optimize the kinetic

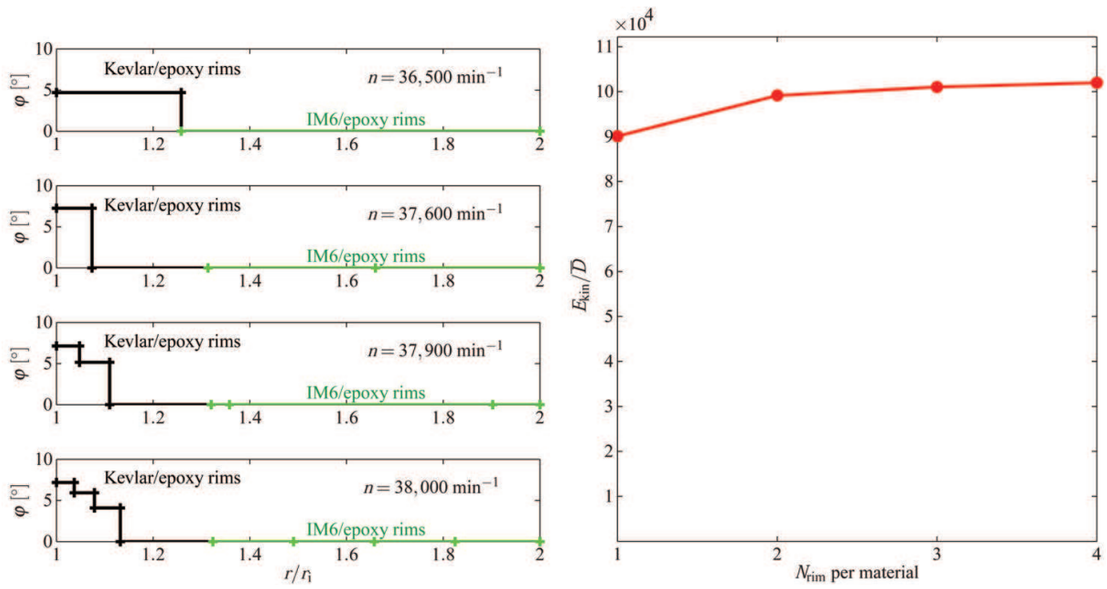

(a) Optimal designs for different numbers of rims (b) Optimal energy-per-cost ratio depending on the number of rims

Fig. 8. Influence of the number of rims per material

energy, cf. Ha et al. (1998).
In Danfelt et al. (1977), the POISSON ratio, the YOUNG modulus and the density were considered as design variables for a flywheel rotor with rubber in between the composite rims. Ha et al. (1998) optimized the design of a single-material multi-rim flywheel rotor with interferences and different fiber angle in each rim. They were able to increase the energy storage capacity by a factor of 2.4 compared to a rotor without interferences and purely circumferentially wound fibers. They also concluded that interferences had more influence on the increase of the overall strength than fiber angle variation. In a following publication, Ha, Yang & Kim (1999) studied the design of a hybrid composite rotor with up to four different materials and optimized the thickness of each rim for different material combinations. Fiber angle variation was also addressed in Fabien (2007). The authors considered the optimization of a continuously varying angle between the radial and the tangential direction for a stacked-ply rotor.
It should be noted that it is also conceivable to optimize the rotor profile, i. e. to vary the height along the radius, see Huang & Fadel (2000a). However, the winding process impedes this type of design optimization in case of an FRPC rotor. Consequently, the height optimization is uncommon to FES using composite materials and instead the ring-type architecture is widely accepted.
In what follows, two design optimization case studies will be presented: (1) The optimization of the discrete fiber angles for a multi-rim hybrid composite rotor and (2) the investigation of the influence of the hub design on the optimum design of a hybrid composite rotor.

4.2.1 Optimum fiber angles for a multi-rim hybrid composite rotor

The effect of fiber angle variation on the optimum energy-per-cost value for a multi-rim hybrid composite rotor with inner Kevlar/epoxy and outer IM6/epoxy rims has been studied. The optimization was carried out for different numbers of rims per material. Due to increased

complexity in manufacturing and assembly the potential for increased expenditure exists with increasing number of different rims. However, such cost-increasing effects were not considered in the modeling. Thus, it is interesting to study the influence of the number of rims on the optimal energy-per-cost value. In **Figures 8(a)** and **8(b)** the results are depicted with (a) their corresponding optimal designs and (b) optimal objective function values. There are only rims with nonzero fiber angles for the Kevlar/epoxy material. The fiber angle is decreasing for increasing radius. The optimal fiber angle for the IM6/epoxy rims is zero. The reason for this is probably that the critical tensile radial stress level in the Kevlar/epoxy rims would be increased by more compliant outer rims. Hence, a non-zero value for the IM6/epoxy fiber angle might lead to delamination failure in this case. Theoretically, it is thus not necessary to increase the number of rims for the IM6/epoxy material to obtain the optimal energy-per-cost ratio. In order to show that the fiber angle still vanishes for additional rims, however, the redundant rims have not been removed in **Figure 8(a)**.

It can be postulated that there is an optimal continuous function for the fiber angle with respect to the radius. In that case, the optimization method would try to fit the discontinuous fiber angle to this continuous function by adjusting the thicknesses and fiber angles of the discrete rims. This assumption is supported by the results of Fabien (2007) which include the computation of an optimal continuous fiber angle distribution. In that reference, however, the fibers are aligned in the radial direction so that the optimization results cannot be compared to the ones in this paper.

As expected, the objective function value increases monotonically with additional design variables. The energy-per-cost value for the configuration with four rims per material exceeds the corresponding value for the single rim configuration by 13%. Since the total thickness of each material remains approximately constant, the normalized cost does not decrease significantly. Thus, the increase in the energy-per-cost ratio is mainly due to the increase of the energy storage capacity. However, it can be seen well from **Figure 8(b)** that the optimal objective converges with increasing numbers of rims per material. Hence, additional manufacturing complexity is not necessarily worthwhile considering the comparatively slow decrease of the energy-per-cost ratio with respect to the number of rims.

4.2.2 Optimization of the hub geometry

The optimization of the hub geometry connected to a two-rim glass/epoxy, carbon/epoxy rotor with $r_\mathrm{i} = 120\,\mathrm{mm}$ and $r_\mathrm{o} = 240\,\mathrm{mm}$ was examined for two common hub types: The conventional ring-type hub and the split-type hub as proposed in Ha et al. (2006). The basic idea of the split-type hub is to interrupt the circumferential stress transmission by splitting up the hub into several segments, facilitating the radial expansion during rotation of the split-ring. This expansion causes compressive hub/rim interface stresses, which makes interference fits or adhesives unnecessary in terms of torque transmission. Furthermore, the compressive hub/rim interface stresses reduce the magnitude of radial tensile stress within the composite rims. Since the radial tensile stress is often the speed-limiting constraint for rotating filament wound composite rings, the energy storage capability can thus be increased. On the other hand, the pressure loading causes increased hoop stresses within the composite rims, which also have the potential of limiting the energy storage capability. Thus, there exists an optimum thickness of the ring part of the hub, as shown in Ha et al. (2006); Krack et al. (2010b). Both hub configurations were considered in the optimization of a hybrid two-rim rotor with prescribed inner and outer rotor diameter. The design variables were the rotational speed n, the inner rim thickness t_1 and the hub thickness t_hub.

	ring-type hub	split-type hub
$\frac{t_1^{\text{opt}}}{t_{\text{all}}}$ [%]	58.28	66.91
n^{opt} [min^{-1}]	46846	44872
$t_{\text{hub}}^{\text{opt}}$ [mm]	0.00	3.80
$\frac{f^{\text{opt}}}{f_{\text{no hub}}^{\text{opt}}}$ [%]	100	103.7

Table 1. Optimization results for different hub architectures with an optimized hub thickness

The optimal hub thickness became zero in the case of the ring-type hub. This means that a ring-type hub generally weakens the strength of the rotor for the given material properties. However, a minimum thickness for the hub ring would be necessary in order to avoid failure and to transmit torque between rotor and shaft. Hence, the results for the optimized ring-type hub with vanishing hub thickness have to be regarded as only theoretical extremal values. For this extreme case, the optimum energy-per-cost value is identical to the one for the case without any hub, i. e., the relative value equals 100%.

On the other hand, an optimal hub thickness of $t_{\text{hub}}^{\text{opt}} = 3.80\,\text{mm}$ was ascertained for the split-type hub. With this optimal design, the energy-per-cost value for the split-type hub is 3.7% higher than for the model with an optimized ring-type hub in this example. Therefore, it is proven that a split-type hub with an optimized thickness enhances the strength of the hybrid composite rotor and thus increases the optimal energy-per-cost value.

4.3 Constraints

The design problem stated in Eq. (13) is constrained by the strength limits of the structure, geometrical bounds and dynamical considerations. Geometrical bounds arise from the design of the surrounding components. A given shaft, hub or casing geometry can restrict the dimensions of the rotor, i. e. the inner and outer radii as well as the axial height. The aspect ratio and the absolute size in conjunction with the bearing properties can also necessitate size constraints in terms of dynamic stability for large rotational speeds, cf. Ha et al. (2008).

The most critical constraints are, however, the structural ones. Various failure criteria have been studied for the design of flywheel rotors. The most common criteria are the Maximum Stress Criterion, the Maximum Strain Criterion and the TSAI-WU Criterion. As the constraints represent the boundary of the feasible region and the optimal designs can typically be found at this boundary, cf. Danfelt et al. (1977), the choice of the failure criterion is essential to the solution of the design problem. The influence of the failure criterion on the optimum design was investigated by Fabien (2007) and Krack et al. (2010c). The stress state in a typical flywheel rotor is dominated by the normal stresses. Thus, the deviations between these failure criteria are often not crucial.

In **Figure 9**, the feasible region for the two design variables, rotational speed n and inner rim thickness $\frac{t_1}{t_{\text{all}}}$ for a two-rim glass/epoxy and carbon/epoxy rotor is illustrated. The feasible region is composed of the nonlinear structural constraints in terms of the Maximum Stress Criterion and the bounds of the thickness. The structural constraints are labeled by their strength ratio R between actual and allowable stress for each composite (glass/epoxy or carbon/epoxy). The first index of the strength ratio corresponds to the coordinate direction ('1' for across the fiber, '2' for in the fiber direction), the second index denotes the sign of the stress ('t' for tensile, 'c' for compressive).

In case of concavely shaped constraint functions, it was shown in Krack et al. (2010c) that

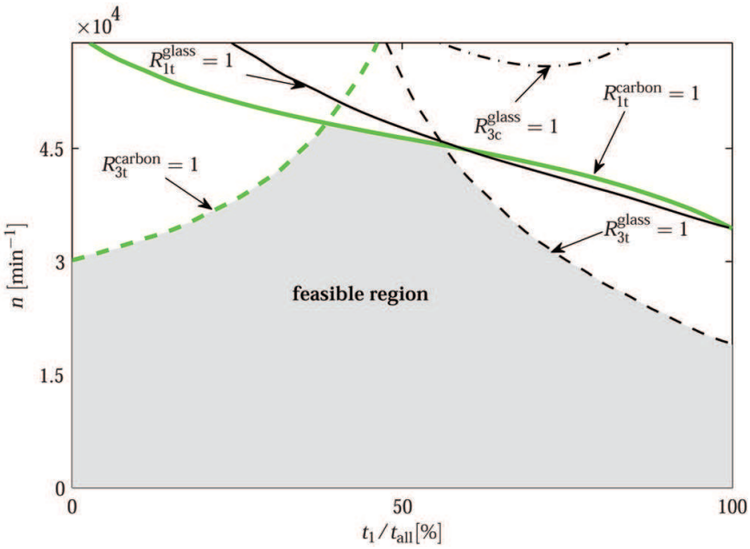

Fig. 9. Composition of the nonlinear constraint for the Maximum Stress Criterion

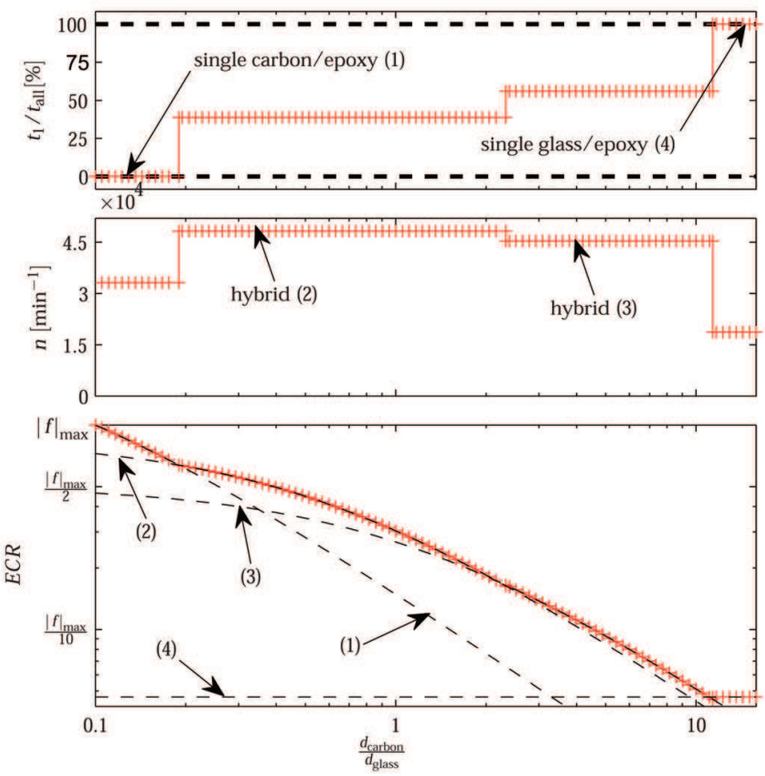

Fig. 10. Optimal designs and objective function values dependent on the cost ratio

in particular the intersecting points of different strength limits that bound the feasible region are candidates for optimal designs. **Figure 10** shows the value of the design variables and objective function at different cost ratios for the hybrid composite flywheel rotor described above. The rotor design was optimized in terms of the energy-per-cost ratio objective ECR, cf. Eq. (19). It is remarkable that the optimum design variables turn out to be discontinuous over

the cost ratio. At specific cost ratios, the optimum thicknesses $\frac{t_1}{t_{\text{all}}}$ and the rotational speed n jump between two different values. Between these jumps, i. e. for wide ranges of the cost ratio, the optimum design variables remain constant in this case.
Four different optimal design sets have to be distinguished according to **Figure 10** depending on the cost ratio interval. At very high or very low cost ratio values, i. e. relatively expensive carbon or glass based composite materials respectively, a single rim rotor with the correspondingly cheaper material is preferable. Hence, a value of $\frac{t_1}{t_{\text{all}}} = 0\,\%$ or $\frac{t_1}{t_{\text{all}}} = 100\,\%$ corresponding to a full carbon/epoxy or a full glass/epoxy material rotor respectively, is obtained. In between these trivial solutions, two additional optimal designs exist.
While the total energy stored and the specific energy density have discrete values for a varying cost ratio, the actual objective, i. e. the optimal energy-per-cost value ECR changes continuously with the cost ratio as illustrated in **Figure 10**. In this figure, the objective function for each of the four design sets is depicted dependent on the cost ratio. Note that the discontinuities of the optimal design variables coincide with intersections of the design-dependent objective function graphs.
It can be concluded from this section that the constraints are essential to the design problem but the decision which design is optimal also depends significantly on the shape of the objective function with respect to the design variables.

4.4 Optimization strategies

Based on the previous discussion, the flywheel design problem in Eq. (13) is a multi-objective, multi-variable nonlinear constrained optimization problem. This section of the chapter discusses possible optimization algorithms that can be used in order to solve such optimization problems. Subsection 4.2 outlined the design variables for the problem which include lay-up materials, fibre angles and thickness, hub geometry and rotational speed. Most of these variables are real variables; therefore this section will focus on optimization strategies for optimization problems with real design variables.
The solution of multi-objective, multi-variable nonlinear constrained optimization problems is a challenging endeavor. First, in a nonlinear optimization problem, there are usually many designs that satisfy the Karush-Kuhn-Tucker (KKT) optimality conditions, see A. Antoniou & W.-S. Lu (2007). All these designs, known as local optima, meet the necessary requirements for optimality, but usually one of these designs will provide better performance than the others. Therefore, the optimization algorithm needs to search not only for an optimal design, but for the optimal design among optimal designs. In addition to the nonlinear nature of the optimization problem, since there are multiple criteria to be optimized, the most optimal design will depend on the relative importance of each one of the design objectives. Therefore, a methodology needs to be used to identify the different trade-offs between design objectives. Finally, optimization problems usually involve a large number of complex numerical simulations, e. g., a detailed multi-dimensional FE simulation of the flywheel. Therefore, it is necessary to select optimization strategies that can minimize the computer resources necessary to solve the design problem.
Subsection 4.4.1 will discuss the advantages and disadvantages of the optimization algorithms that can be used to solve nonlinear constraint optimization problems. Subsection 4.4.2 provides an overview of multi-objective optimization and presents two alternative methods that can be used to solve such problems. Finally, Subsection 4.4.3 will present several methodologies that have recently been used in order to reduce computational resources.

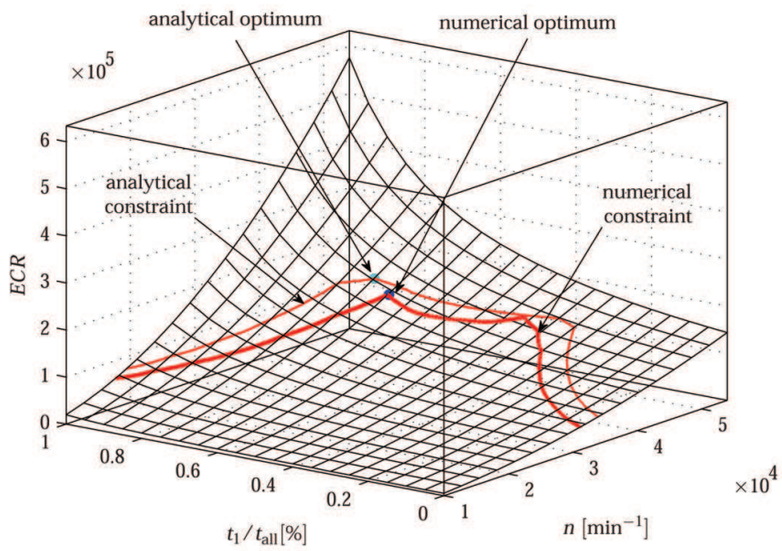

Fig. 11. Objective function and analytical and numerical nonlinear constraints depending on the relative inner rim thickness t_1/t_{all} and the rotational speed n

4.4.1 Constraint optimization algorithms

As discussed, for many nonlinear optimization design problems, multiple local optima may exist which makes solving the optimization problem more difficult. **Figure 11** shows the design space for the flywheel optimization problem solved by Krack et al. (2010c). It can be observed in **Figure 11** that there are two points that can be considered optimal solutions, i.e. $(n, t_1/t_{all}) = (4.25 \times 10^4, 0.4)$ and $(n, t_1/t_{all}) = (4.0 \times 10^4, 0.7)$. Therefore, even for monotonic objective functions and a small number of design variables multiple local optima occur due to the introduction of strongly nonlinear constraints. Hence, it is important to verify that the optimum detected by a specific method is a global optimum and not only a local one.

Nonlinear constraint optimization algorithms can be classified as local methods and global methods. Local methods aim to obtain a local minimum, and they cannot guarantee that the minimum obtained is the absolute one. These methods are usually first-order methods, i.e. they require information about the gradient of the objective function and the constraints. The most commonly used local methods include the method of feasible directions (MFD) and the modified method of feasible directions (MMFD) (see Arora (1989); Vanderplaats (1984)); sequential linear programming (SLP) (see Arora (1989); Lamberti & Pappalettere (2000); Vanderplaats (1984)); sequential quadratic programming (SQP) (see A. Antoniou & W.-S. Lu (2007)); nonlinear interior point methods (see A. Antoniou & W.-S. Lu (2007); El-Barky et al. (1996)), and; response surface approximation methods (RSM) (see Rodríguez et al. (2000); Wang (2001)). Local methods are prone to finding an optimum in the nearby region of the initial starting guess; however, these methods work very efficiently in the vicinity of the optimum.

Global methods aim at obtaining the global minimum. These methods do not require any information about the gradient, and they employ primarily either a stochastic-based or an heuristic-based algorithm. Therefore, the use of global methods can reduce the likelihood of missing the global optimum. (Albeit there is no guarantee of finding the global optimum.) Global methods, however, have the disadvantage of requiring far more function evaluations. Particularly in the case of computationally expensive function evaluations, e. g. nonlinear FE

analyses with a large number of elements, global methods are often not applicable in practice. Global methods either solve the constraint nonlinear problem directly, or they transform the problem into an unconstrained problem using a penalty method (see Vanderplaats (1984) for a description of common penalty methods). Common optimization algorithms that solve the constrained problem directly include covering methods and pure random searches. If the constrained optimization problem is transformed into an unconstrained one, common unconstrained global optimization problems include genetic algorithms (see Goldberg (1989)), evolutionary algorithms (see Michalewicz & Schoenauer (1996)) and simulated annealing (see Aarts & Korst (1990)).

Although local methods do not aim at obtaining a global optimum, several approaches can be used to continue searching once a local minimum has been obtained, thereby enabling the identification of all local minima. Once all local minima have been obtained, it is easy to identify the global minimum. Some of these methods are: random multi-start methods (e.g., He & Polak (1993); Schoen (1991)), ant colony searches (e.g., Dorigo et al. (1996)) and local-minimum penalty method (e.g., Ge & Qin (1987)).

Another approach to obtaining a global solution when the computational resources are limited is to combine a global and a local optimization algorithm. Global optimization algorithms are usually relatively quick at obtaining a solution that is near the global optimum; however, they are usually slow at converging to an optimal solution that meets the optimality conditions. In order to reduce computational resources during the later stages of finding an optimal solution, a global optimization algorithm can be used during the initial stages of the solution of the design problem. Then, the sub-optimal solution obtained by the global optimization algorithm can be used as the initial guess to the local method. Since local optimization algorithms usually converge very quickly to the optimal solution, a reduction in computational resources can usually be achieved. Further, since the initial solution was already in the vicinity of the global optimum, it is likely that the local optimization algorithm will converge to the global optimum. This approach was recently used to design a hybrid composite flywheel by Krack et al. (2010c). In order to show the benefits of the proposed multi-strategy scheme, the optimization problem was solved with a global method, i.e. an evolutionary algorithm (EA), a local method, i.e. a nonlinear interior-point method (NIPM), and the multi-strategy scheme, i.e. start with EA algorithm and switch to the interior-point method after a relatively flexible convergence criteria was achieved. Krack et al. (2010c) showed that the multi-strategy scheme was 35% faster than the global method.

4.4.2 Multi-objective optimization algorithms

The optimization formulation in Eq. (13) contains multiple objectives that need to be optimized simultaneously such as kinetic energy stored, mass and cost. In the late-nineteenth-century, Edgeworth and Pareto showed that, in most multi-objective problems, an *utopian* solution that minimizes all objectives simultaneously cannot be obtained because some objectives are conflicting. Therefore, the scalar concept of optimality does not apply directly to design problems with multiple objectives that need to be optimized simultaneously.

A useful notion in multi-objective problems is the concept of *Pareto optimality*. A design, $\vec{x}$, is a *Pareto optimal solution* for problem (13), if and only if the solution $\vec{x}^*$ cannot be changed to improve one of the objectives without adversely affecting at least one other objective (Ngatchou et al. (2005)). Based on this definition, Pareto optimality solutions, $\vec{x}^*$, are non-unique. The *Pareto optimal set* is defined as the set that contains all Pareto optimal

solutions. Furthermore, the *Pareto front* is the set that contains the objectives of all optimal solutions.

Since all Pareto optimal solutions are good solutions, the most appropriate solution will depend only upon the trade-offs between objectives; therefore, it is the responsibility of the designer to choose the most appropriate solution. It is sometimes desirable to obtain the complete set of Pareto optimal solutions, from which the designer may then choose the most appropriate design.

There is a large number of algorithms for solving multi-objective problems, see e.g. Das & Dennis (1998); Kim & de Weck (2005; 2006); Lin (1976); Messac & Mattson (2004); Ngatchou et al. (2005). These methods can be classified between: a) classical approaches; and, b) meta-heuristic approaches as proposed by Ngatchou et al. (2005). Classical approaches are based on either transforming the multiple objectives into a single aggregated objective or optimizing one objective at a time, while the other objectives are treated as constraints. Examples of classical methods are the weighted sum method and the ε-constraint method (see Ngatchou et al. (2005)). In the weighted sum method (e.g., Kim & de Weck (2006)), the multiple objectives are transformed into a single objective function by multiplying each objective by a weighting factor and summing up all contributions such that the final objective is:

$$F_{weighted\,sum} = w_1 f_1 + w_2 f_2 + \cdots + w_n f_n \tag{20}$$

where f_i are the objective functions, w_i are the weighting factors and $\sum_i w_i = 1$. Each single set of weights determines one Pareto optimal solution. A Pareto front is obtained by solving the single objective optimization problem with different combinations of weights. The weighted sum method is easy to implement; however it has two drawbacks: 1) a uniform spread of weight parameters rarely produces a uniform spread of points on the Pareto set; 2) non-convex parts of the Pareto set cannot be obtained, (see Das & Dennis (1997)).

Meta-heuristic methods are population-based methods using genetic or evolutionary algorithms. Meta-heuristic methods aim at generating the Pareto front directly by evaluating, for a given population, all design objectives simultaneously. For each population, all designs are ranked in order to retain all Pareto optimal solutions. The main advantage of these methods is that many potential solutions that belong to the Pareto set can be obtained in one single run. Examples of multi-objective meta-heuristic methods include the multi-objective genetic algorithm (MOGA), the non-dominated sorting genetic algorithm (NSGA) and the strength Pareto evolutionary algorithm (SPEA). A detailed description of these methods can be found in Ngatchou et al. (2005) and Veldhuizen & Lamont (2000).

Multi-objective optimization of flywheels has recently been attempted by Huang & Fadel (2000b) and Krack et al. (2010b). In both cases, the weighted sum method was used in order to solve the optimization problem. Huang and Fadel aimed at maximizing kinetic energy storage while minimizing the difference between maximum and minimum Von Mises stresses for an alloy flywheel with different cross-sectional areas. The flywheel was divided into several rims and the design variables were the height of each rim in the flywheel. Krack et al. (2010b) aimed at maximizing kinetic energy storage while minimizing cost. Stress within the flywheel was included as a constraint in the optimization problem. In their case, the flywheel was a composite flywheel with several rims and the design variables were the thickness of each rim and the flywheel rotational speed.

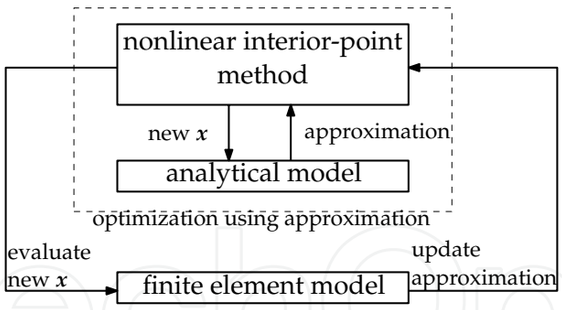

Fig. 12. Schematic of a multi-fidelity simulation. The high-fidelity finite element simulation is called to correct the lower-fidelity analytical model

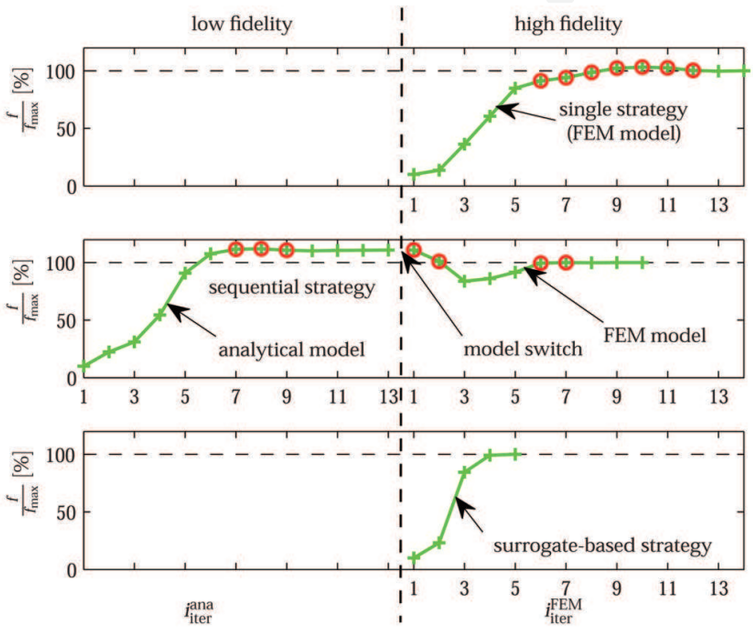

Fig. 13. Convergence histories of the cost optimization of a hybrid composite flywheel rotor with a split-type hub for different optimization strategies

4.4.3 Multi-fidelity and surrogate-based optimization

Accurate predictions of stress and strain in variable geometry flywheels and hubs require solving a set of complex multi-dimensional partial differential equations (PDEs). The system of PDEs is usually solved using the finite element method (FEM). Multi-dimensional FEM simulations of complex geometries require a substantial amount of computational resources. Further, since in order to solve a flywheel optimization problem many flywheel designs will need to be evaluated, the computational expense associated with flywheel design and optimization is a major challenge for solving such problems.

In order to reduce the computational resources associated with solving optimization problems, optimization strategies based on combining analysis tools of different accuracy have emerged in the literature (see Alexandrov et al. (2000); Forrester & Keane (2009); Simpson et al. (2001)). In multi-fidelity and surrogate-based optimization strategies, the optimization method only iterates on an approximate model. The multi-dimensional flywheel model is then used sporadically in order to apply a correction to the approximation. In multi-fidelity

models, the approximation is usually a simplified version, i.e. a lower fidelity model, of the original problem such as a one-dimensional simplification of the multi-dimensional flywheel problem. In surrogate-based optimization, the approximation or meta-model, called a surrogate, is simply a fit to numerical or experimental data and, therefore, it is not based on the physics of the problem. Various approaches exist to construct a surrogate model, including the commonly used polynomial response surface models (RSM) and neural networks. Many of them are described in great detail in references Forrester & Keane (2009); Simpson et al. (2001).

Krack et al. (2010b) used a multi-fidelity approach to minimize the computational time required to solve a flywheel optimization problem. A variant of the approximation model management framework (AMMF) proposed by Queipo et al. (2005) was used in order to solve the problem. In this case, the optimization is performed using the low fidelity model and the FEM model is used to correct the low fidelity model for accuracy. The correction, a first order polynomial that is added to the solution of the low fidelity model, is obtained using the FEM model. The correction guarantees that the low fidelity model matches the FEM predictions for the design objective and constraints and its gradients at a specified design point. A schematic of the interaction between the low and high fidelity model is shown in **Figure 12**. The optimization algorithm uses information from the low fidelity model to obtain the optimal solution. After the optimal solution using the low fidelity model has been obtained, a correction polynomial is obtained using FEM and a new optimization problem is solved in the corrected low fidelity model. This process is repeated until both FEM and low fidelity model result in the same optimal design. In reference Krack et al. (2010b), using the multi-fidelity approach the computational resources were reduced three fold from 3,025 sec. to 1,087 sec. **Figure 13** compares the convergence history of three different strategies to solving the problem: a) using only a high-fidelity model; b) using the low- and high-fidelity models sequentially, i.e. solve the optimization problem using the low-fidelity model and then, use the solution as the initial design for a new optimization problem with the high-fidelity model; and, c) the multi-fidelity approach. Red circles indicate infeasible designs. Using the multi-fidelity model involves the least number of evaluations of the high-fidelity model.

5. Conclusion

An overview of rotor design for state-of-the-art FES systems was given. Practical design aspects in terms of manufacturing have been discussed. Typical analytical and FE modeling approaches have been presented and their suitability for the design optimization process regarding accuracy and computational efficiency has been investigated. The design of a hybrid composite flywheel rotor was formulated as a multi-objective, multi-variable nonlinear constrained optimization problem. Well-proven approaches to the solution of the design problem were presented and thoroughly discussed. The capabilities of the suggested methodology were demonstrated for various numerical examples.

6. References

A. Antoniou & W.-S. Lu (2007). *Practical Optimization: Algorithms and Engineering Applications*, Springer.

Aarts, E. & Korst, J. (1990). *Simulated annealing and Boltzmann machines*, Vol. 7, Wiley Chichester.

Alexandrov, N., Lewis, R., Gumbert, C., Green, L. & Newman, P. (2000). Optimization with variable-fidelity models applied to wing design, *AIAA paper* 841(2000): 254.

Arnold, S. M., Saleeb, A. F. & Al-Zoubi, N. R. (2002). Deformation and life analysis of composite flywheel disk systems, *Composites Part B: Engineering* 33(6): 433–459.

Arora, J. (1989). *Introduction to optimum design*, McGraw-Hill.

Arvin, A. & Bakis, C. (2006). Optimal design of press-fitted filament wound composite flywheel rotors, *Composite Structures* 72(1): 47–57.

Bornemann, H. J. & Sander, M. (1997). Conceptual system design of a 5 mwh/100 m w superconducting flywheel energy storage plant for power utility applications, *IEEE Transactions on Applied Superconductivity* 7(2 PART 1): 398–401.

Brown, D. R. & Chvala, W. D. (2005). Flywheel energy storage: An alternative to batteries for UPS systems, *Energy Engineering: Journal of the Association of Energy Engineering* 102(5): 7–26.

Christopher, D. A. & Donet, C. (1998). Flywheel technology and potential benefits for aerospace applications, *IEEE Aerospace Applications Conference Proceedings*, Vol. 1, pp. 159–166.

Danfelt, E., Hewes, S. & Chou, T. (1977). Optimization of composite flywheel design, *International Journal of Mechanical Sciences* 19: 69–78.

Das, I. & Dennis, J. (1997). A closer look at drawbacks of minimizing weighted sums of objectives for Pareto set generation in multicriteria optimization problems, *Structural Optimization* 14: 63–69.

Das, I. & Dennis, J. (1998). Normal-boundary intersection: a new method for generation pareto optimal points in multicriteria optimization problems, *SIAM Journal of Optimization* 8: 631–657.

Dorigo, M., Maniezzo, V. & Colorni, A. (1996). Ant system: optimization by a colony of cooperating agents, *Systems, Man, and Cybernetics, Part B: Cybernetics, IEEE Transactions on* 26(1): 29–41.

El-Barky, A., Tapia, R., Tshchiya, T. & Zhang, Y. (1996). On the formulation and theory of the newton interior point method for nonlinear programming, *Journal of Optmization Theory and Applications* 89(3): 507–541.

Fabien, B. (2007). The influence of failure criteria on the design optimization of stacked-ply composite flywheels, *Structural and Multidisciplinary Optimization* 33(6): 507–517.

Forrester, A. I. & Keane, A. J. (2009). Recent advances in surrogate-based optimization, *Progress in Aerospace Sciences* 45(1-3): 50–79.

Gabrys, C. W. & Bakis, C. E. (1997). Design and manufacturing of filament wound elastomeric matrix composite flywheels, *Journal of Reinforced Plastics and Composites* 16(6): 488–502.

Ge, R. & Qin, Y. (1987). A class of filled functions for finding global minimizers of a function of several variables, *Journal of Optmization Theory and Applications* 54(2): 241–252.

Genta, G. (1985). *Kinetic energy storage: theory and practice of advanced flywheel systems*, Butterworth and Co. Ltd, London.

Goldberg, D. (1989). *Genetic algorithms in search, optimization, and machine learning*, Addison-Wesley.

Gowayed, Y., Abel-Hady, F., Flowers, G. & Trudell, J. (2002). Optimal design of multi-direction composite flywheel rotors, *Polymer composites* 23(3): 433–441.

Ha, S., Jeong, H. & Cho, Y. (1998). Optimum design of thick-walled composite rings for an energy storage system, *Journal of composite materials* 32(9): 851–873.

Ha, S. & Jeong, J. (2005). Effects of winding angles on through-thickness properties and residual strains of thick filament wound composite rings, *Composites Science and technology* 65(1): 27–35.

Ha, S., Kim, D. & Choi, S. (1999). Optimal design of a hybrid composite flywheel rotor using finite element methods, *Evolving and revolutionary technologies for the new millennium* 44: 2119–2132.

Ha, S., Kim, D. & Sung, T. (2001). Optimum design of multi-ring composite flywheel rotor using a modified generalized plane strain assumption, *International journal of mechanical sciences* 43(4): 993–1007.

Ha, S., Kim, H. & Sung, T. (2003). Measurement and prediction of process-induced residual strains in thick wound composite rings, *Journal of Composite Materials* 37(14): 1223–1237.

Ha, S., Kim, J. & Han, Y. (2008). Design of a Hybrid Composite Flywheel Multi-rim Rotor System using Geometric Scaling Factors, *Journal of Composite Materials-Lancaster* 42(8): 771–786.

Ha, S., Kim, M., Han, S. & Sung, T. (2006). Design and Spin Test of a Hybrid Composite Flywheel Rotor with a Split Type Hub, *Journal of Composite Materials* 40(23): 2113–2130.

Ha, S., Yang, H. & Kim, D. (1999). Optimal design of a hybrid composite flywheel with a permanent magnet rotor, *Journal of Composite Materials* 33(16): 1544–1575.

He, L. & Polak, E. (1993). Multistart method with estimation scheme for global satisfying problems, *Journal of Global Optimization* 3: 139–156.

Hebner, R., Beno, J. & Walls, A. (2002). Flywheel batteries come around again, *IEEE spectrum* 39(4): 46–51.

Huang, B. C. (1999). Polar woven flywheel rim design, *International SAMPE Symposium and Exhibition (Proceedings)*, Vol. 44, p. II/.

Huang, J. & Fadel, G. (2000a). Heterogeneous flywheel modeling and optimization, *Materials and Design* .

Huang, J. & Fadel, G. (2000b). Heterogeneous flywheel modeling and optimization, *Materials and Design* 21(2): 111–125.

Kim, I. & de Weck, O. (2005). Adaptive weighted sum method for bi-objective optimization: pareto front generation, *Structural and Multidisciplinary Optimization* 29: 149–158.

Kim, I. & de Weck, O. (2006). Adaptive weighted sum method for multiobjective optimization: a new method for pareto front generation, *Structural and Multidisciplinary Optimization* 31: 105–116.

Krack, M., Secanell, M. & Mertiny, P. (2010a). Advanced optimization strategies for cost-sensitive design of energy storage flywheel rotors, *International SAMPE Symposium and Exhibition (Proceedings)* .

Krack, M., Secanell, M. & Mertiny, P. (2010b). Cost optimization of a hybrid composite flywheel rotor with a split-type hub using combined analytical/numerical models, *Structural and Multidisciplinary Optimization* pp. 1–17.

Krack, M., Secanell, M. & Mertiny, P. (2010c). Cost optimization of hybrid composite flywheel rotors for energy storage, *Structural and Multidisciplinary Optimization* 41(5): 779–796.

Lamberti, L. & Pappalettere, C. (2000). Comparison of the numerical efficiency of different sequential linear programming based algorithms for structural optimization problems, *Computers and Structures* 76(6): 713–728.

Lin, J. G. (1976). Multiple-objective problems: pareto-optimal solutions by method of proper equality constraints, *IEEE Transactions on Automatic Control* 21(5): 641–650.

Messac, A. & Mattson, C. A. (2004). Normal constraint method with guarantee of even representation of complete pareto frontier, *AIAA Journal* 42(10): 2101–2111.

Michalewicz, Z. & Schoenauer, M. (1996). Evolutionary algorithms for constrained parameter optimization problems, *Evolutionary computation* 4(1): 1–32.

Motor Trend (1952). the GYROBUS: Something New Under the Sun?, *Motor Trend* p. 37.

Ngatchou, P., Anahita Zarei & El-Sharkawi, M. (2005). Pareto Multi Objective Optimization, *Proceedings of the 13th International Conference on Intelligent Systems Application to Power Systems* art. no. 1599245: 84-91.

Portnov, G. G. (n.d.). *Composite flywheels, In: Handbook of Composites, Structures and Design Vol. 2*, Elsevier Science Publishers, Amsterdam.

Queipo, N. V., Haftka, R. T., Shyy, W., Goel, T., Vaidyanathan, R. & Tucker, P. K. (2005). Surrogate-based analysis and optimization, *Progress in Aerospace Sciences* 41(1): 1–28.

Ratner, J. K. H., Chang, J. B. & Christopher, D. A. (2003). Composite flywheel rotor technology - a review, *ASTM Special Technical Publication*, pp. 3–28.

Rodríguez, J., Renaud, J., Wujek, B. & Tappeta, R. (2000). Trust region management is multidisciplinary design optimization, *Journal of Computational and Applied Mathematics* 124: 139–154.

Schoen, F. (1991). Stochastic techniques for global optimization: A survey of recent advances, *Journal of Global Optimization* 1(3): 207–228.

Secanell, M., Songprakorp, R., Suleman, A. & Djilali, N. (2008). Multi-objective optimization of a polymer electrolyte fuel cell membrane electrode assembly, *Energy and Environmental Science* 1(3): 378–388.

Simpson, T., Peplinski, J., Koch, P. & Allen, J. (2001). Metamodels for computer-based engineering design: Survey and recommendations, *Engineering with Computers* 17(2): 129–150.

Takahashi, K., Kitade, S. & Morita, H. (2002). Development of high speed composite flywheel rotors for energy storage systems, *Advanced Composite Materials* 11(1): 40–49.

Tarrant, C. (1999). Revolutionary flywheel energy storage system for quality power, *Power Engineering Journal* 13(3): 159–163.

Tsai, S. (1988). Composite design, *Think Composites* 1: 1–19.

Tzeng, J. (2003). Viscoelastic analysis of composite rotor for pulsed power applications, *IEEE Transactions on Magnetics* 39(1): 384–388.

Tzeng, J., Emerson, R., Moy, P. & MD, A. R. L. A. P. G. (2005). *Composite Flywheel Development for Energy Storage*, Defense Technical Information Center.

Vanderplaats, G. (1984). *Numerical optimization techniques for engineering design with applications*, McGraw-Hill.

Veldhuizen, D. & Lamont, G. (2000). Multiobjective evolutionary algorithms: analyzing the state-of-the-art., *Evolutionary computation* 8(2): 125–147.

Wang, G. (2001). Improvement on the Adaptive Response Surface Method for High-Dimensional Computation-Intensive Design Problems, *ASME Design Engineering Technical Conferences–Design Automation Conference*.

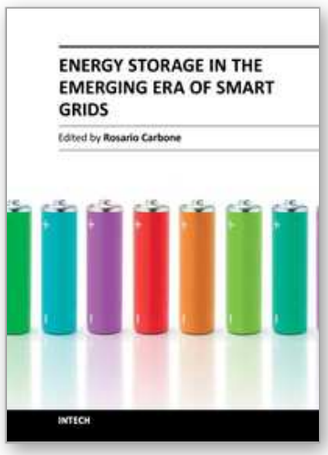

Energy Storage in the Emerging Era of Smart Grids

Edited by Prof. Rosario Carbone

ISBN 978-953-307-269-2
Hard cover, 478 pages
Publisher InTech
Published online 22, September, 2011
Published in print edition September, 2011

Reliable, high-efficient and cost-effective energy storage systems can undoubtedly play a crucial role for a large-scale integration on power systems of the emerging â€œdistributed generationâ€ (DG) and for enabling the starting and the consolidation of the new era of so called smart-grids. A non exhaustive list of benefits of the energy storage properly located on modern power systems with DG could be as follows: it can increase voltage control, frequency control and stability of power systems, it can reduce outages, it can allow the reduction of spinning reserves to meet peak power demands, it can reduce congestion on the transmission and distributions grids, it can release the stored energy when energy is most needed and expensive, it can improve power quality or service reliability for customers with high value processes or critical operations and so on. The main goal of the book is to give a date overview on: (I) basic and well proven energy storage systems, (II) recent advances on technologies for improving the effectiveness of energy storage devices, (III) practical applications of energy storage, in the emerging era of smart grids.

How to reference

In order to correctly reference this scholarly work, feel free to copy and paste the following:

Malte Krack, Marc Secanell and Pierre Mertiny (2011). Rotor Design for High-Speed Flywheel Energy Storage Systems, Energy Storage in the Emerging Era of Smart Grids, Prof. Rosario Carbone (Ed.), ISBN: 978-953-307-269-2, InTech, Available from: http://www.intechopen.com/books/energy-storage-in-the-emerging-era-of-smart-grids/rotor-design-for-high-speed-flywheel-energy-storage-systems

INTECH
open science | open minds

InTech Europe
University Campus STeP Ri
Slavka Krautzeka 83/A
51000 Rijeka, Croatia
Phone: +385 (51) 770 447
Fax: +385 (51) 686 166
www.intechopen.com

InTech China
Unit 405, Office Block, Hotel Equatorial Shanghai
No.65, Yan An Road (West), Shanghai, 200040, China
中国上海市延安西路65号上海国际贵都大饭店办公楼405单元
Phone: +86-21-62489820
Fax: +86-21-62489821

IntechOpen